

# Cascade calculations of X-ray yields in kaonic hydrogen and deuterium

T.S. Jensen

6 March 2003

## Abstract

The X-ray yields in kaonic hydrogen and deuterium have been calculated in the extended standard cascade model for different values of the strong interaction parameters. The dependence of the yields on the  $1s$  shifts and widths is moderate. For a given  $2p$  strong interaction width, the yields in kaonic hydrogen and deuterium are expected to be of similar magnitude.

## 1 Introduction

A detailed understanding of the atomic cascade is important for the planning and interpretation of experiments in kaonic hydrogen and deuterium. For example, reliable theoretical predictions of the absolute X-ray yields are needed in order to determine the optimal experimental conditions for achieving the highest count rates. In addition, predictions of relative  $K$  yields are useful for the data analysis of the  $K$  X-ray spectrum as a cascade constrained fit can lead to an improved determination of the  $1s$  width.

Cascade model predictions of  $K^-p$  and  $K^-d$  X-ray yields have been published in Refs. [1, 2]. The X-ray yields presented in this Note are calculated in the extended standard cascade model which has a number of significant improvements over the earlier calculations [3].

This Note is organized as follows: in Sect. 2 the extended standard cascade model is described. The calculated X-ray yields in kaonic hydrogen and deuterium are presented in Sect. 3 and the conclusion is given in Sect. 4.

## 2 Theory

### 2.1 Extended standard cascade model

The extended standard cascade model (ESCM), which was developed in the recent years, is described in detail in Ref. [3]. The ESCM is used to simulate the cascade in exotic atoms with  $Z = 1$  by taking the different cascade processes listed in Table 1 into account. The cascade program uses an ensemble of 100000+ exotic atoms initially formed in highly excited states and calculates the life history of each as they cascade down through the  $nl$  states and the kinetic energy changes through

collisional acceleration (Coulomb deexcitation) and deceleration. A significant advantage of the ESCM compared to earlier cascade studies is obtained by the use of new results for the collisional processes [3]. In the upper part of the cascade ( $n > 10$  for  $K^-p$ ) a classical-trajectory Monte Carlo model has been used to calculate simultaneously Coulomb, Stark, and elastic collisions for scattering from hydrogen *molecules*. The detailed calculations of the collisions at high  $n$  replace the so-called chemical deexcitation or molecular dissociation which was introduced by Leon and Bethe [4] (and used in later cascade models, for example Ref. [1]) as a phenomenological solution to the problem of the measured cascade times. In the lower part of the cascade a quantum mechanical description of the exotic atom is applied for calculating the collisional processes. The target hydrogen is treated as consisting of individual *atoms* for reasons of simplification.

Process	Example
Stark transitions:	$(K^-p)_{nl_i} + \text{H}_2 \rightarrow (K^-p)_{nl_f} + \text{H}_2^*$
External Auger effect:	$(K^-p)_i + \text{H} \rightarrow (K^-p)_f + p + e^-$
Coulomb deexcitation:	$(K^-p)_{n_i} + \text{H}_2 \rightarrow (K^-p)_{n_f} + \text{H}_2^*, \quad n_f < n_i$
Elastic scattering:	$(K^-p)_{nl} + \text{H}_2 \rightarrow (K^-p)_{nl} + \text{H}_2^*$
Absorption:	$(K^-p)_i + \text{H} \rightarrow \pi^0 + \Lambda + \text{H}$
Radiative transitions:	$(K^-p)_{n_i l_i} \rightarrow (K^-p)_{n_f l_f} + \gamma$
Nuclear reactions:	$(K^-p)_{ns} \rightarrow \pi^0 + \Lambda$
Decays:	$K^- \rightarrow \mu^- \bar{\nu}_\mu$

Table 1: Processes included in the extended standard cascade model.

Based on the new results for the cascade processes, it is found that the atomic cascade in  $K^-p$  in a typical hydrogen gas target will proceed as follows:

- $n = 25 \rightarrow 10$ : Coulomb deexcitation (chemical deexcitation).
- $n = 10 \rightarrow \sim 6$ : external Auger effect, nuclear absorption.
- $n = \sim 6 \rightarrow 1$ : external Auger effect, nuclear absorption, Coulomb deexcitation, radiative transitions.

## 2.2 Strong interaction shift/width

The strong interaction shifts and widths affect the absorption during the cascade and therefore the X-ray yields. In kaonic hydrogen and deuterium the important strong interaction parameters are the  $1s$  shift ( $\Delta E_{1s}^{\text{had}}$ ), the  $1s$  width ( $\Gamma_{1s}^{\text{had}}$ ), and the  $2p$  width ( $\Gamma_{2p}^{\text{had}}$ ). The shifts/widths for higher  $ns$  and  $np$  states can be obtained using the formulas

$$\Gamma_{ns}^{\text{had}} = \frac{\Gamma_{1s}^{\text{had}}}{n^3}, \quad (1)$$

$$\Gamma_{np}^{\text{had}} = \frac{32(n^2 - 1)}{3n^5} \Gamma_{2p}^{\text{had}} \quad (2)$$

and similarly for the shifts.

The effect of the  $1s$  shift/width can be estimated in a simple way as follows. We use the two-state approximation where the second state (that is the  $ns$  state) is shifted by

$$\epsilon = E - \frac{i}{2}\Gamma \quad (3)$$

compared to the first state which is assumed to be stable. We want to estimate the strength of absorption from the first state when a small perturbation which mixes the states is introduced. The potential energy matrix is given by

$$\mathbf{V} = \begin{pmatrix} 0 & V \\ V & \epsilon \end{pmatrix}$$

where  $V = V(r)$  is the distance dependent interaction causing transitions between the states. For  $E > 0$  the relevant adiabatic energy curve is given by

$$V_{\text{ad}}(r) = \frac{1}{2} \left( \epsilon - \sqrt{\epsilon^2 + 4V(r)^2} \right) . \quad (4)$$

Assuming that the perturbation is small,  $|V| \ll |\epsilon|$ , we find to lowest order

$$\text{Im}(V_{\text{ad}}) \propto \frac{\Gamma}{E^2 + (\Gamma/2)^2} . \quad (5)$$

From the properties of this function (5) it follows that for fixed  $E$  the absorption is maximal for

$$\Gamma = 2E \quad (6)$$

and vanishes for  $\Gamma \rightarrow \infty$ . The absolute yields in hadronic atoms are, therefore, expected to have a minimum around  $\Gamma = 2E$  for fixed  $E$ . This result is confirmed by the calculations in kaonic deuterium, Sect. 3.2.

### 3 X-ray yields

The cascade program requires that the initial state of the exotic hydrogen atom is specified. In this Note we use:  $n_i = 25$ , statistical distribution in  $l_i$ , and an average kinetic energy of 0.5 eV (Maxwell distribution). The X-ray yields in density range under experimental consideration are, however, virtually insensitive to the initial state.

The cascades in  $K^-p$  and  $K^-d$  are expected to be very similar provided that the strong interaction parameters are the same because the scales involved in the cascade processes, such as the dissociation and ionization energy of  $\text{H}_2$  vs.  $\text{D}_2$  molecules and the energy spacing between energy levels of the exotic atom, are similar for  $K^-p$  and  $K^-d$ .

#### 3.1 Kaonic hydrogen

We use the central values of the result from KEK for the  $1s$  strong interaction shift and width [5]:

$$\Delta E_{1s}^{\text{had}} = 323 \pm 63(\text{stat}) \pm 11(\text{sys}) \text{ eV} , \quad (7)$$

$$\Gamma_{1s}^{\text{had}} = 407 \pm 208(\text{stat}) \pm 100(\text{sys}) \text{ eV} . \quad (8)$$

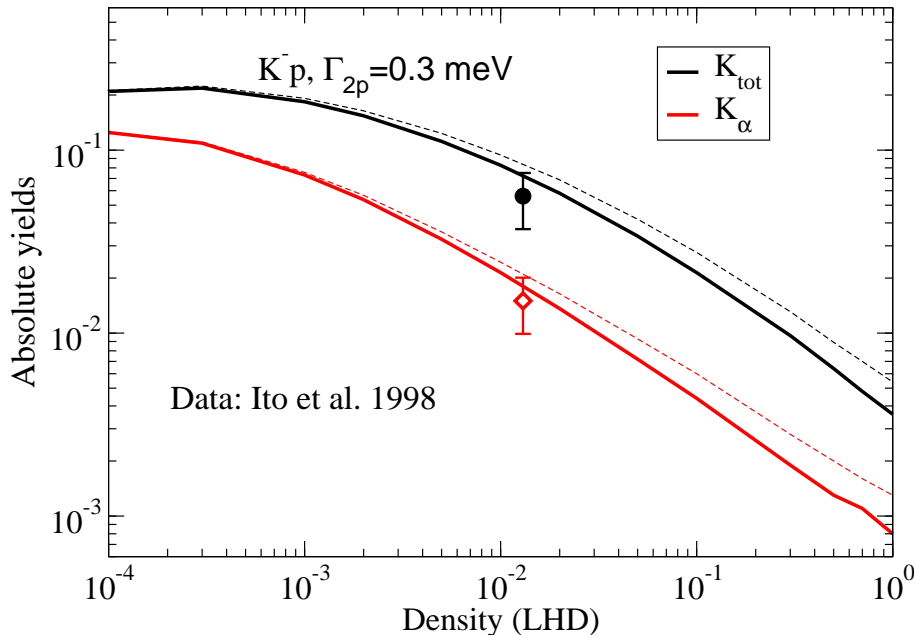


Figure 1: The absolute X-ray yields,  $K_{\text{tot}}$  and  $K_{\alpha}$ , in kaonic hydrogen. The experimental result is from [6]. The thin dashed lines are the results obtained with cross sections calculated in the fixed field model.

The  $2p$  strong interaction width  $\Gamma_{2p}^{\text{had}}$  is poorly known. Unless otherwise indicated, we use

$$\Gamma_{2p}^{\text{had}} = 0.3 \text{ meV} \quad (9)$$

which is consistent with  $KN$  scattering data.

Figure 1 shows the density dependence of the absolute X-ray yields,  $K_{\text{tot}}$  and  $K_{\alpha}$ , in kaonic hydrogen. The yields decrease with increasing density as collisional absorption becomes more efficient. Below 0.001 LHD<sup>1</sup> the effect of kaon weak decay can be seen: the cascade time becomes comparable with the kaon life time and many kaonic atoms do not reach the lower  $n$  states. The yields are in good agreement with the result of the KEK experiment [6]. Using the cross section calculated in the fixed field model (see Ref. [3]) results in yields that are somewhat higher, for example 14% higher at 0.01 LHD for the total  $K$  yield.

The density dependence of the relative yields  $K_x/K_{\text{tot}}$  is shown in Fig. 2. At low densities ( $< 0.01$  LHD) the  $K_{\alpha}$  line is dominant, for higher densities several  $K$  X-ray lines have comparable intensity. For both the absolute and relative yields there is qualitative agreement with the results of the cascade calculations in Ref. [1].

Figure 3 shows the predicted  $K$  X-ray intensities at 0.013 LHD compared with the cascade-unconstrained fit of the KEK spectrum [6]. The agreement is very good for the  $K_{\alpha}$  and the  $K_{\beta}$  yields. The error bars resulting from the fit for the higher lines are highly correlated so no conclusion is possible here.

Figure 4 shows the dependence of the total yield  $K_{\text{tot}}$  on the  $2p$  strong interaction width for different densities. The calculated yields decrease as the absorption from the  $np$  states become increasingly efficient. Figure 5 shows the  $\Gamma_{2p}^{\text{had}}$  dependence of

<sup>1</sup>Densities are given in units of liquid hydrogen density (LHD).

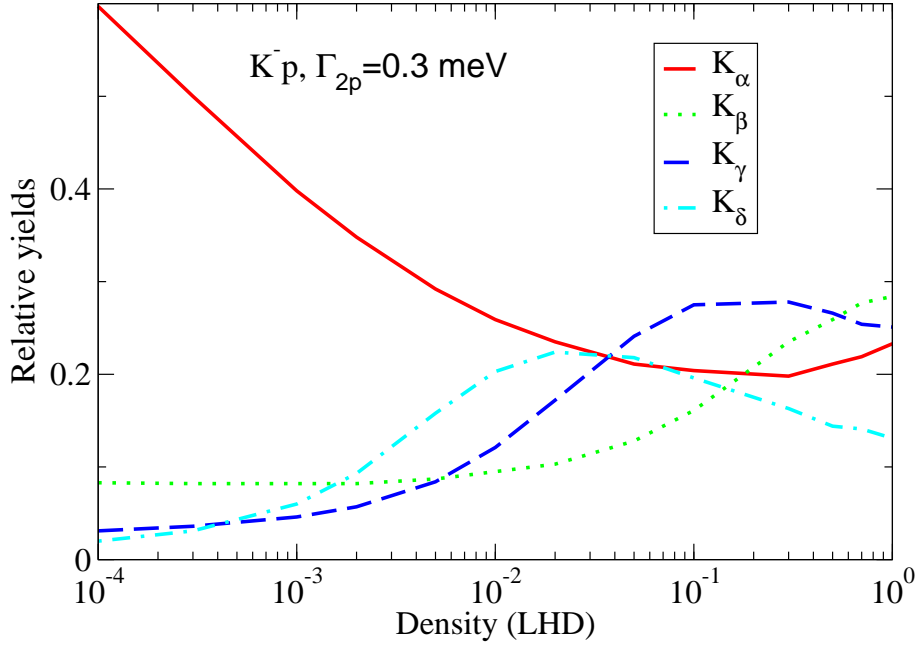


Figure 2: The relative  $K$  X-ray yields in kaonic hydrogen.

the relative yield  $K_\alpha/K_{\text{tot}}$ . The relative yield is small for large  $\Gamma_{2p}^{\text{had}}$  as the strong absorption rate dominates the  $2p \rightarrow 1s$  radiative rate. The  $\Gamma_{2p}^{\text{had}}$  dependence of the relative vs. absolute  $K_\alpha$  and  $K_\beta$  yields is shown for different densities in Figs. 6, 7, and 8. The only experimental data available so far, Fig. 6, suggest a strong interaction width  $\Gamma_{2p}^{\text{had}} \sim 0.2 - 0.5$  meV. The calculated  $K$  yields can be found in Table 2 (0.013 LHD) and Table 3 (0.031 LHD).

One can estimate the theoretical errors of the cascade calculation by introducing tuning parameters multiplying the various cross sections used as input. In the case of X-ray yields, the largest uncertainty comes from the collisional absorption and Stark mixing. The parameter  $k_A$  is multiplied with the cross section for absorption during collision, Stark and elastic transitions and varied between 0.5 and 1.5. The results for the X-ray yields are shown in Table 4. The prediction for the absolute yield is most uncertain, that of the relative  $K_\alpha$  yield much less. The ratio  $K_\alpha/L_{\text{tot}}$  can be predicted with even higher certainty. As all three quantities depend on the  $2p$  width, the two ratios are most suitable for determining  $\Gamma_{2p}^{\text{had}}$ . Further studies show that the theoretical error of the absolute yield increases for higher densities and/or smaller  $\Gamma_{2p}^{\text{had}}$ .

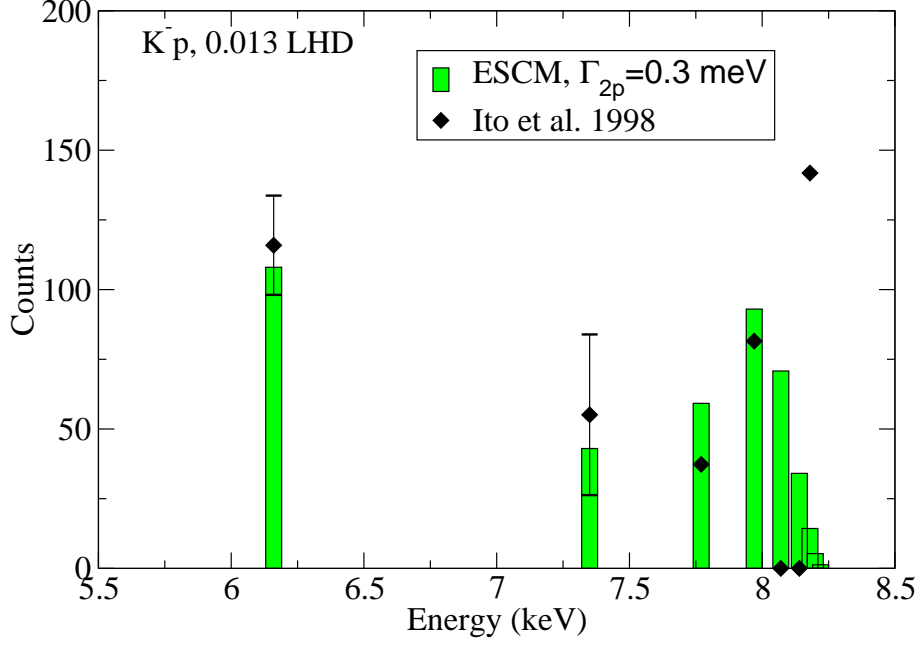


Figure 3: The kaonic hydrogen  $K$  X-ray intensities at 0.013 LHD. Filled diamonds: the results of the fit from [6]. The error bars are only shown for the  $K_\alpha$  and  $K_\beta$  lines as they are highly correlated for the higher lines. Bars: the result of the ESCM with  $\Gamma_{2p}^{\text{had}} = 0.3$  meV normalized to the measured total yield.

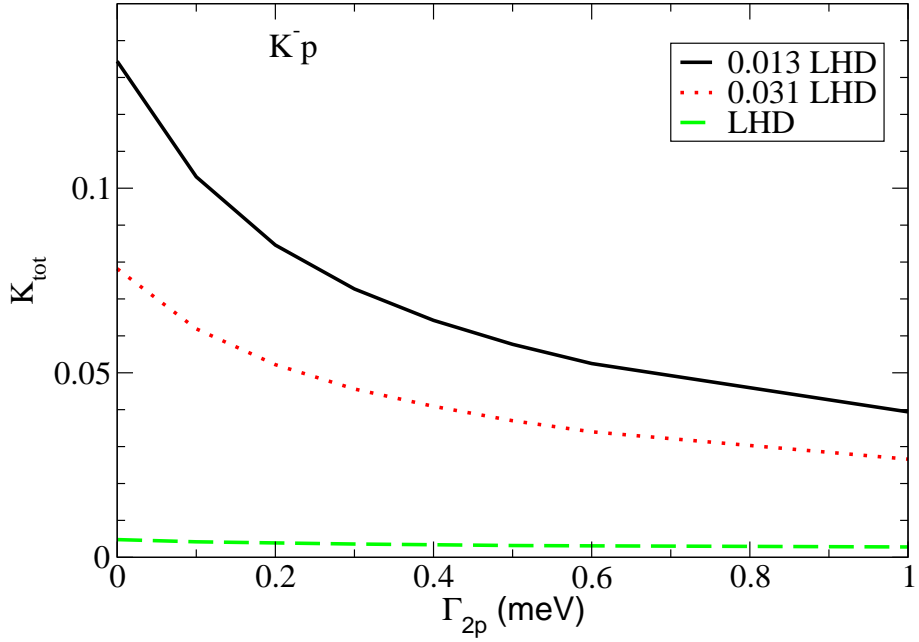


Figure 4: The  $\Gamma_{2p}^{\text{had}}$  dependence of the total yield  $K_{\text{tot}}$  in  $K^-p$ .

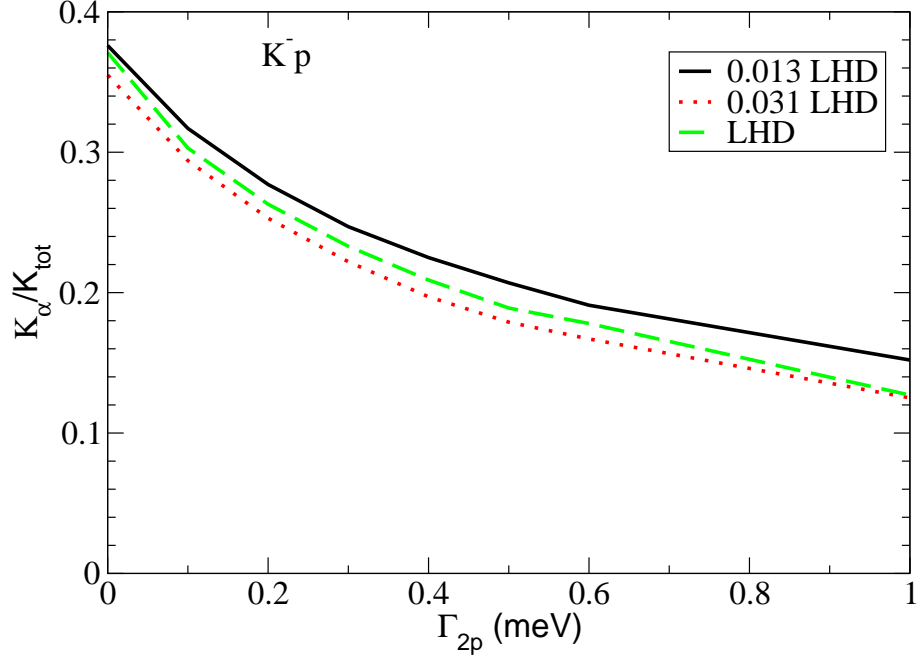


Figure 5: The  $\Gamma_{2p}^{\text{had}}$  dependence of the relative yield  $K_\alpha/K_{\text{tot}}$  in  $K^-p$ .

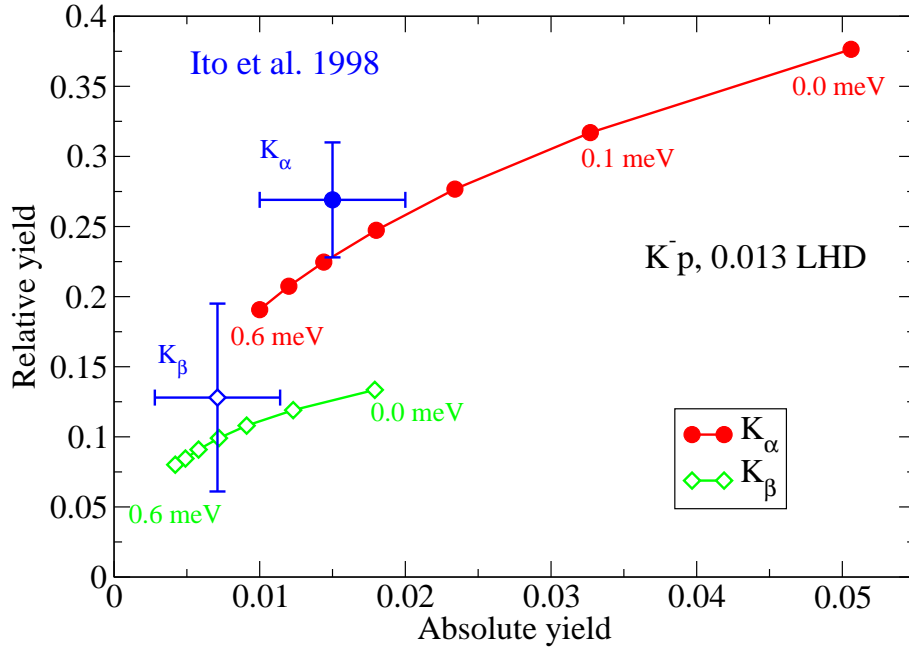


Figure 6: The relative vs. absolute  $K$  yields in  $K^-p$  at 0.013 LHD. The  $2p$  width is given by 0.0, 0.1, 0.2, 0.3, 0.4, 0.5, and 0.6 meV. The experimental result is from [6].

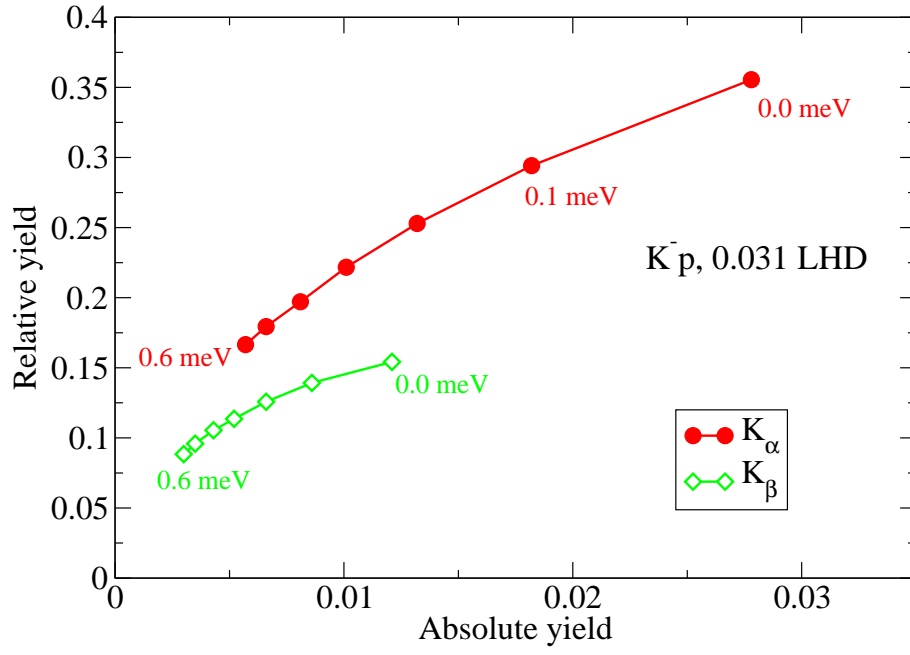


Figure 7: The relative vs. absolute  $K$  yields in  $K^-p$  at 0.031 LHD. The  $2p$  width is given by 0.0, 0.1, 0.2, 0.3, 0.4, 0.5, and 0.6 meV.

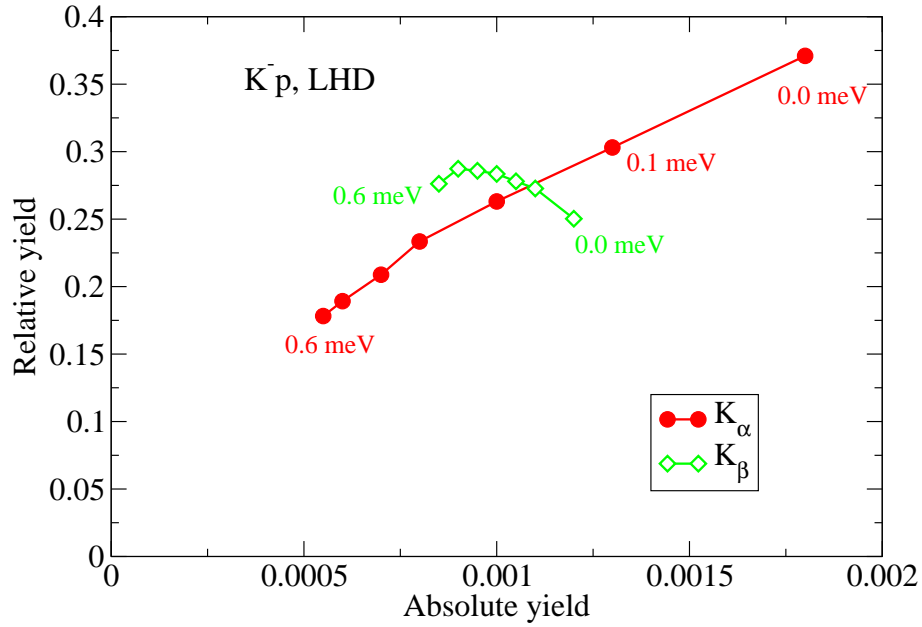


Figure 8: As Fig. 7 in liquid hydrogen.



$n$	$\Gamma_{2p}$						
	0.0	0.1	0.2	0.3	0.4	0.5	0.6
2	5.01	3.26	2.36	1.81	1.44	1.18	1.01
3	1.82	1.24	0.93	0.71	0.58	0.48	0.41
4	1.99	1.53	1.22	1.01	0.84	0.72	0.62
5	2.17	1.93	1.74	1.56	1.42	1.30	1.21
6	1.38	1.34	1.26	1.22	1.16	1.12	1.06
7	0.64	0.61	0.58	0.58	0.58	0.56	0.55
8	0.24	0.24	0.24	0.24	0.24	0.22	0.22
9	0.09	0.09	0.09	0.09	0.09	0.09	0.09

Table 2: The kaonic hydrogen  $K$  X-ray yields ( $np \rightarrow 1s$ ) in % at 0.013 LHD for  $n = 2 - 9$ . The  $2p$  strong interaction width is in meV.

$n$	$\Gamma_{2p}$						
	0.0	0.1	0.2	0.3	0.4	0.5	0.6
2	2.77	1.82	1.32	1.01	0.80	0.67	0.56
3	1.20	0.86	0.66	0.53	0.42	0.36	0.31
4	1.52	1.27	1.07	0.93	0.82	0.73	0.66
5	1.24	1.15	1.09	1.01	0.97	0.92	0.88
6	0.66	0.64	0.64	0.62	0.60	0.60	0.58
7	0.27	0.28	0.27	0.26	0.26	0.26	0.26
8	0.10	0.10	0.10	0.10	0.10	0.10	0.10
9	0.04	0.04	0.04	0.04	0.04	0.04	0.04

Table 3: The kaonic hydrogen  $K$  X-ray yields ( $np \rightarrow 1s$ ) in % at 0.031 LHD for  $n = 2 - 9$ . The  $2p$  strong interaction width is in meV.

Yield	$k_A$		
	0.5	1.0	1.5
$K_{\text{tot}}$	0.120	0.074	0.051
$K_\alpha/K_{\text{tot}}$	0.288	0.247	0.231
$K_\alpha/L_{\text{tot}}$	0.400	0.387	0.381

Table 4: The kaonic hydrogen  $K$  X-ray yields at 0.013 LHD for  $\Gamma_{2p}^{\text{had}} = 0.3$  meV. The tuning parameter is given by  $k_A = 0.5, 1.0, 1.5$ .

### 3.2 Kaonic deuterium

The  $K^- - d$  strong interaction has been studied by Barrett and Deloff [7] using phenomenological fits to low-energy ( $NK, Y\pi$ ) data. Both the shift and width of the  $1s$  state are expected to be around 1 keV. In this Note we use

$$\Delta E_{1s} = 500 \text{ eV} , \quad (10)$$

$$\Gamma_{1s}^{\text{had}} = 1000 \text{ eV} . \quad (11)$$

The various predictions of the  $2p$  strong interaction width are in disagreement with each other. Among the published results are:

- $\Gamma_{2p}^{\text{had}} = 46 \text{ meV}$ . Assuming  $p$  state absorption occurs through  $s$  wave  $NK$  interaction [7].
- $\Gamma_{2p}^{\text{had}} = 0.014 \text{ meV}$ . This estimate is an improvement compared to the former and is based on the Deser-Trueman formula for the  $L = 1$  case [7].
- $\Gamma_{2p}^{\text{had}} = 25 \text{ meV}$ . Obtained by solving the Klein-Gordon equation with an optical potential fitted to heavier ( $Z \geq 3$ ) kaonic atom data [1].
- $\Gamma_{2p}^{\text{had}} = (4 \pm 2.3) \text{ meV}$ . Estimated using Fermi pseudo potentials and isotopic invariance [2].

The widths should be compared to the  $2p \rightarrow 1s$  radiative width

$$\Gamma^{\text{rad}}(2p \rightarrow 1s) = 0.3 \text{ meV} . \quad (12)$$

The  $2p$  strong interaction width has a strong influence on the predicted yields and it is crucial for the planning of future experiments to understand the origin of these discrepancies. In the following, we will use

$$\Gamma_{2p}^{\text{had}} = 1.0 \text{ meV} . \quad (13)$$

The cascade calculations in kaonic deuterium differ from the hydrogen case in that the cross sections for absorption during collisions and Stark and elastic collisions were obtained in the numerically less involved fixed field model. As shown for  $K^-p$  in Fig. 1 this means that the absolute yields are somewhat overestimated.

The calculated X-ray yields for kaonic deuterium shown in Figs. 9 and 10 are qualitatively similar to the  $K^-p$  ones (Figs. 1 and 2). The relative yield  $K_\alpha/K_{\text{tot}}$  is suppressed in  $K^-d$  compared to the  $K^-p$  case because of the larger  $2p$  strong interaction width used.

Figure 11 shows the dependence of the  $K$  X-ray yields on the  $1s$  shift,  $\Delta E_{1s}$ , at 0.013 LHD. The yields increase monotonically with increasing  $1s$  shift as expected. The dependence of the  $K$  X-ray yields on the  $1s$  width is shown in Fig. 12. The dependence is strongest for  $\Gamma_{1s}^{\text{had}} < \Delta E_{1s}$  while for  $\Gamma_{1s}^{\text{had}} > 2\Delta E_{1s}$  the yields remain nearly constant.

Figure 13 shows the  $\Gamma_{2p}^{\text{had}}$  dependence of the X-ray yields,  $K_{\text{tot}}$ ,  $K_\alpha$ , and  $K_\alpha/K_{\text{tot}}$ . The results are very similar to the kaonic hydrogen case.

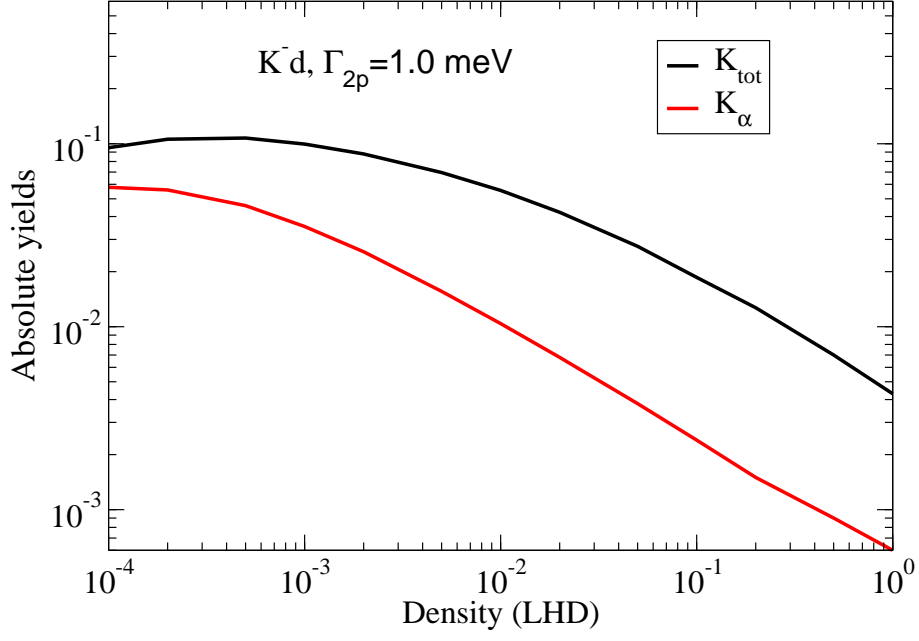


Figure 9: The density dependence of the absolute  $K$  X-ray yields in kaonic deuterium.

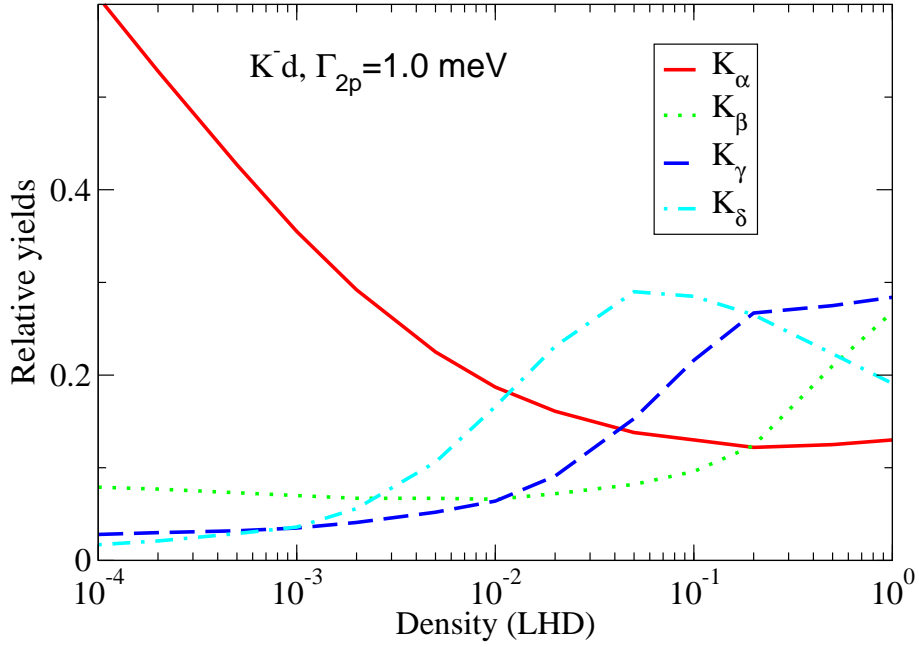


Figure 10: The density dependence of the relative  $K$  X-ray yields in kaonic deuterium.

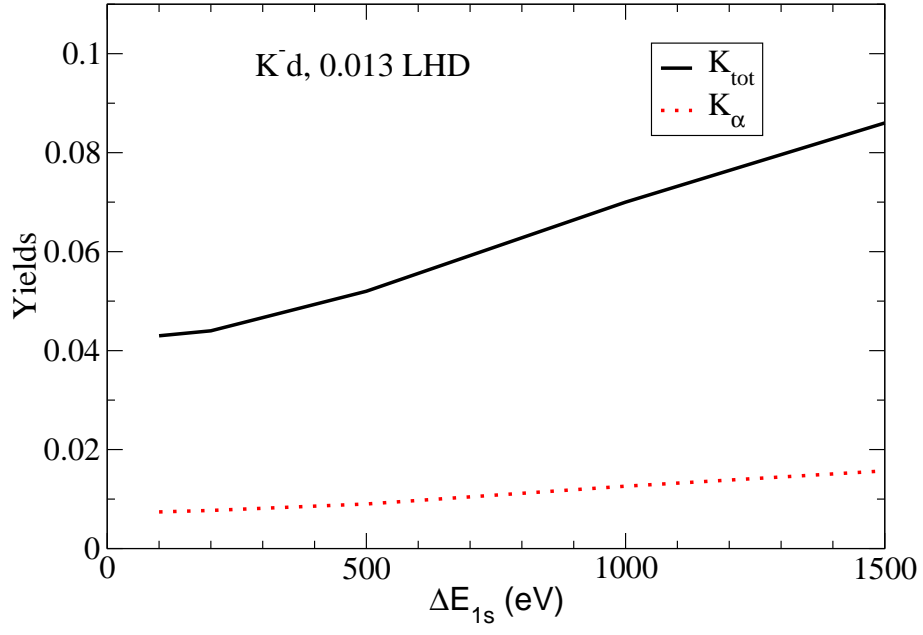


Figure 11: The  $\Delta E_{1s}$  dependence of the X-ray yields in kaonic deuterium at 0.013 LHD.

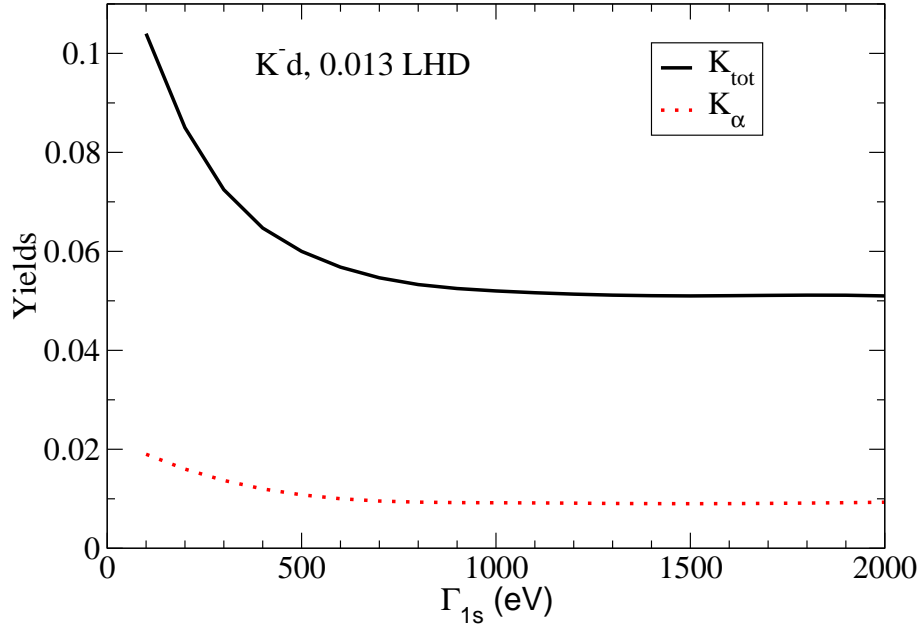


Figure 12: The  $\Gamma_{1s}^{\text{had}}$  dependence of the X-ray yields in kaonic deuterium at 0.013 LHD.

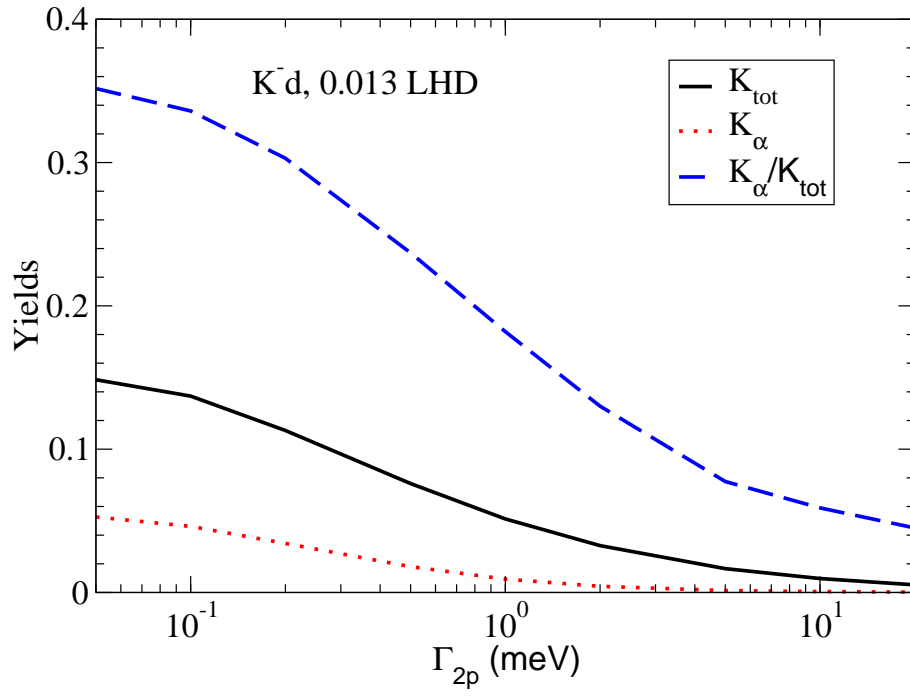


Figure 13: The  $\Gamma_{2p}^{\text{had}}$  dependence of the X-ray yields in kaonic deuterium at 0.013 LHD.

## 4 Conclusion

The X-ray yields in kaonic hydrogen and deuterium have been calculated in the extended standard cascade model. The dependence on the target density and the strong interaction shifts and widths has been investigated. The findings can be summarized as follows:

- There is a moderate dependence of the absolute yields on the  $1s$  shift and width. For a given shift  $\Delta E_{1s}$  the absolute yield has a minimum for  $\Gamma_{1s}^{\text{had}} \sim 2|\Delta E_{1s}|$ . The relative  $K_\alpha$  yield is nearly insensitive to the  $1s$  shift and width.
- Both the absolute and relative  $K_\alpha$  yields decrease strongly with increasing  $2p$  strong interaction width. The relative yield  $K_\alpha/K_{\text{tot}}$  is less sensitive than the absolute yield to uncertainties in the cascade calculations and is suitable for determining the  $2p$  width.
- The cascades in  $K^-p$  and  $K^-d$  are very similar for the same set of strong interaction parameters. The X-ray intensities are expected to be of the same magnitude provided that the  $2p$  widths are approximately equal.

The extended standard cascade model will improve in the future as better theoretical calculations of the cross sections (for example taking molecular effects into account at low  $n$ ) are used and new experimental data on X-ray yields and kinetic energy distributions become available for comparison.

## References

- [1] T. Koike, T. Harada, and Y. Akaishi, Phys. Rev. C **53**, 79 (1996).
- [2] M.P. Faifman *et al.*, Frascati Phys. Series **XVI**, 637 (1999).
- [3] T.S. Jensen and V.E. Markushin, Eur. Phys. J. D **19**, 165 (2002); **21**, 261 (2002); **21**, 271 (2002).
- [4] M. Leon and H.A. Bethe, Phys. Rev. **127**, 636 (1962).
- [5] M. Iwasaki *et al.*, Phys. Rev. Lett. **78**, 3067 (1997).
- [6] T.M. Ito *et al.*, Phys. Rev. C **58**, 2366 (1998).
- [7] R.C. Barrett and A. Deloff, Phys. Rev. C **60**, 025201 (1999).